Mott Transition and Transport Crossovers in the Organic Compound κ – (B E D T – T T F) 2 C u [N (C N) 2] C l

P. Limelette, P. Wzietek, S. Florens, A. Georges, T. Costi, C. Pasquier, D. Jerome, C. Meziere, P. Batail

Mott Transition and Transport Crossovers in the Organic Compound κ-(BEDT-TTF)$_2$Cu[N(CN)$_2$]Cl

P. Limelette,[1] P. Wzietek,[1] S. Florens,[2,1] A. Georges,[2,1] T. A. Costi,[3] C. Pasquier,[1] D. Jérome,[1] C. Mézière,[4] and P. Batail[4]

[1]*Laboratoire de Physique des Solides (CNRS, U.R.A. 8502), Bâtiment 510, Université de Paris-Sud, 91405 Orsay, France*
[2]*LPT-Ecole Normale Supérieure (CNRS-UMR 8549), 24, rue Lhomond, 75231 Paris Cedex 05, France*
[3]*Institut für Theorie der Kondensierten Materie, Universität Karlsruhe, 76128 Karlsruhe, Germany*
[4]*Laboratoire Chimie Inorganique, Matériaux et Interfaces (CIMI), FRE 2447 CNRS, Université d'Angers, 49045 Angers, France*

(Received 27 January 2003; published 2 July 2003)

We have performed in-plane transport measurements on the two-dimensional organic salt κ-(BEDT-TTF)$_2$Cu[N(CN)$_2$]Cl. A variable (gas) pressure technique allows for a detailed study of the changes in conductivity through the insulator-to-metal transition. We identify four different transport regimes as a function of pressure and temperature (corresponding to insulating, semiconducting, "bad metal," and strongly correlated Fermi-liquid behaviors). Marked hysteresis is found in the transition region, which displays complex physics that we attribute to strong spatial inhomogeneities. Away from the critical region, good agreement is found with a dynamical mean-field calculation of transport properties using the numerical renormalization group technique.

DOI: 10.1103/PhysRevLett.91.016401 PACS numbers: 71.30.+h, 74.70.Kn, 74.25.Fy

The Mott metal-insulator transition (MIT) is a key phenomenon in the physics of strongly correlated electron materials. It has been the subject of extensive experimental studies in transition metal oxides, such as $(V_{1-x}Cr_x)_2O_3$ or chalcogenides such as $NiS_{2-x}Se_x$ (for a review, see Ref. [1]). In contrast to chemical composition, hydrostatic pressure allows in principle a continuous sweeping through the transition. For these materials, however, the appropriate range of pressure is several kilobars. For this reason, many fundamental aspects of the MIT are yet to be studied in detail. This issue is particularly important in view of recent theoretical predictions for, e.g., spectroscopy and transport close to the transition, which should be put to experimental test [2]. Layered charge-transfer salts of the κ-(BEDT-TTF)$_2X$ family (where X is a monoanion) offer a remarkable opportunity for such a study. Indeed, these compounds are known to display a great sensitivity to hydrostatic pressure [3]. The κ-(BEDT-TTF)$_2$Cu[N(CN)$_2$]Cl compound, in particular, (abbreviated κ-Cl below) displays a very rich phase diagram with paramagnetic insulating, antiferromagnetic insulating, superconducting, and metallic phases when pressure is varied over a range of a few hundred bars [3–5].

In this Letter, we report on an extensive experimental study of the in-plane resistivity of the κ-Cl compound for a range of pressure spanning both the insulating and the metallic phases. In contrast to previous studies [3], pressure is varied continuously using a helium gas cell, at constant temperature. By analyzing the pressure and temperature dependence of the measured resistivity, we have identified important crossover lines, which are summarized on the phase diagram of Fig. 1. These crossovers separate four different regimes of transport (to be described below) within the paramagnetic phase, corresponding to an "insulator," a "semiconductor," a "bad metal," and a Fermi-liquid metallic regime. Our measurements were performed both with increasing and decreasing pressure sweeps, yielding a determination of the two spinodal lines $P_1^c(T)$ and $P_2^c(T)$ shown in Fig. 1 (see also Fig. 3 below).

A critical comparison is made to dynamical mean-field theory (DMFT [2]), which describes successfully the observed transport crossovers, while the critical region

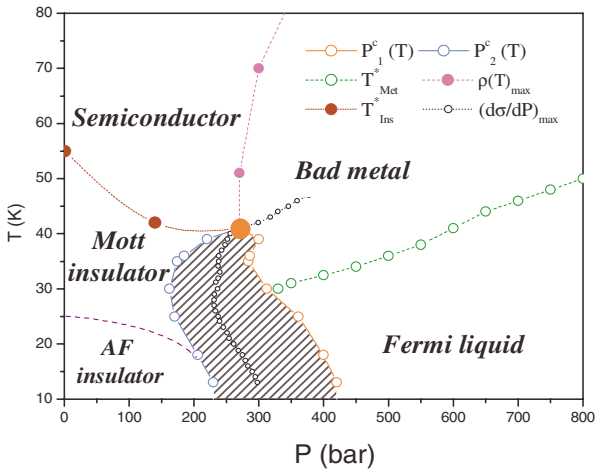

FIG. 1 (color online). Pressure-temperature phase diagram of the κ-Cl salt. The crossover lines identified from our transport measurements delimit four regions, as described in the text. The spinodal lines defining the region of coexistence of insulating and metallic phases (hatched) are indicated, as well as the line where $d\sigma/dP$ is maximum. The latter yields an estimate of the first-order transition line, ending in a critical end point. The transition line into an antiferromagnetic insulating phase has been taken from Ref. [5], while the superconducting phase [3,5] below 13 K has been omitted.

itself reveals more complex behavior. Numerical renormalization group (NRG) calculations of the resistivity within DMFT are reported here for the first time, and compare favorably to the experimental data.

This paper is based mainly on the data set displayed in Fig. 2. The in-plane conductivity was measured using a standard four-terminal method as a function of pressure between 1 bar and 1 kbar. The temperature range 13–52 K was investigated, with pressure sweeps performed every Kelvin (for clarity, only selected temperatures are displayed in Fig. 2). The data clearly demonstrate how pressure drives the system from a low-conductivity insulating regime at low pressure (below 200 bar) to a high-conductivity metallic regime at high pressure (above 350 bar), with a more complex transition region in the 200–350 bar range.

The pressure interval in which the normalized difference between these two measurements exceeds our experimental precision (inset of Fig. 3) corresponds to the region of coexistence between the insulating and metallic phases. This interval is found to be rather large ($\sim$ 100 bar) at 35 K, and still measurable (although the signal is close to our error bars) at 39 K. Note that a much narrower interval would be found from the width at half-maximum. We emphasize that varying pressure rather than temperature is a much more accurate experimental technique for the investigation of the coexistence region, because of the shape of the spinodal lines in the (P, T) plane. This also ensures a better accuracy on pressure (of order 1 bar) as compared to a cooling experiment. Our measurements yield a determination of the critical point in the $T_c \simeq 39$ K to $T_c \simeq 42$ K range ($P_c \simeq 280$ bar), somewhat higher than previously reported from NMR [5] or sound velocity [6] experiments. The data in Fig. 3 are far from the "ideal" situation of a sharp discontinuity in $\sigma(p)$ for $T < T_c$, and present rather a wide region of phase coexistence, in which the measured $\sigma(P)$ displays sizable noise. This suggests a complex physics in this regime, with the likely appearance of insulating and metallic domains in the material, and pinning by disorder.

We now focus on the low-pressure, insulating regime. At low temperature (below 50 K), an activation law $\rho \sim \exp(\Delta/2T)$ describes the data quite well. The temperature range over which this activation law applies is limited both from below and from above. Indeed, at the lowest temperatures a transition into the antiferromagnetic insulating phase is found (around 25 K at ambient pressure, see Fig. 1), while a crossover to a different insulating regime is observed at higher temperatures, as discussed below. Despite this limited range, a reasonable determination of the insulating gap Δ in the "paramagnetic insulator" region of Fig. 1 can be achieved, since $\Delta \gg T$. An approximately linear pressure dependence (see Fig. 4) is found: $\Delta \simeq 740 - 2P_{\mathrm{bar}}$ (in Kelvin). Hence, the activation gap is still *a large scale* close to the coexistence region ($\Delta \simeq 400$ K at 150 bar), of the order of 10 times the critical temperature associated with the transition. Δ cannot be reliably determined above 150 bar, but a rough extrapolation would lead to a gap closure around 370 bar, on the *high-pressure side* of the coexistence region of Fig. 1, suggesting that the finite-temperature Mott transition in this material is *not driven* by the closure of the Mott gap. At higher temperature (above $T \simeq 50$ K at ambient pressure), the T dependence of the resistivity deviates from the above activation law (inset of Fig. 4). This crossover into a "semiconducting" regime, which extends over much of the high-T part of the phase diagram, is indicated in Fig. 1. Interestingly, the crossover scale is *an order of magnitude smaller* than the insulating gap.

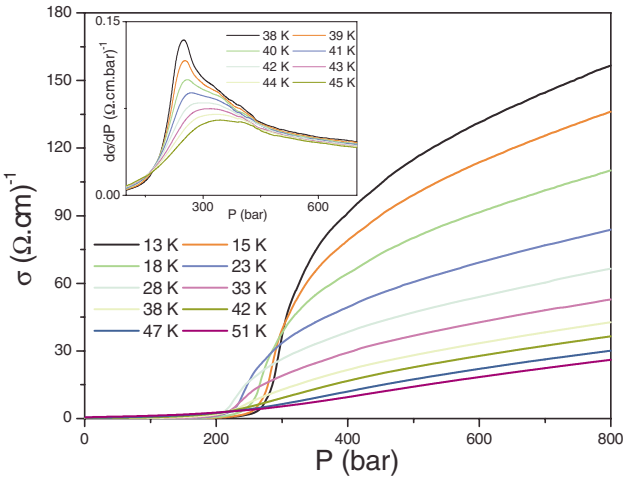

FIG. 2 (color online). Pressure dependence of the in-plane conductivity σ at different temperatures. The inset shows the derivative $d\sigma/dP$ which reveals a sharp peak at low temperature.

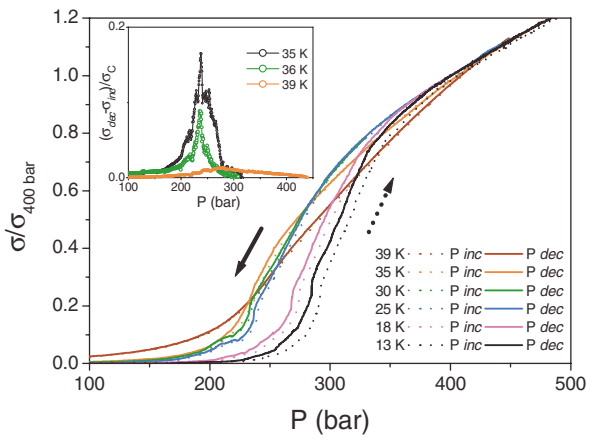

FIG. 3 (color online). Conductivity measured for increasing (σ_{inc}) and decreasing (σ_{dec}) pressure sweeps, at different temperatures up to 39 K. Hysteresis at 35 and 39 K is more apparent in the difference $\sigma_{\mathrm{dec}} - \sigma_{\mathrm{inc}}$ (inset).

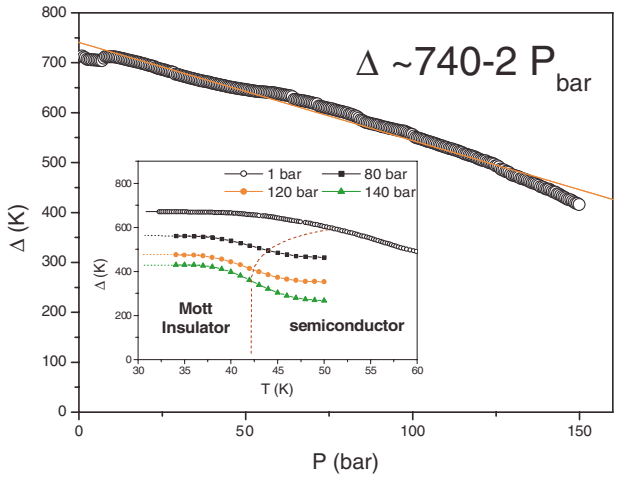

FIG. 4 (color online). Pressure dependence of the paramagnetic gap. The inset displays $\Delta = 2d\ln\rho/d(1/T)$ vs T for a few pressures, from which the crossover from a Mott insulator to a semiconductor is identified.

The high pressure regime above 300 bar is now considered. As demonstrated in the right inset of Fig. 5, the resistivity in this regime has a quadratic, Fermi-liquid dependence upon temperature at low temperatures: $\rho = \rho_0(P) + A(P)T^2$. The quality of the fit, obtained by replotting the data set of Fig. 2 as a function of T^2, illustrates the high precision of the variable pressure technique. The coherence temperature T^* above which this law is no longer valid (of the order of 35 K at 500 bar) defines the onset of a bad metal regime, as indicated in Fig. 1. The prefactor $A(P)$ of the T^2 dependence is found to depend strongly on pressure, as displayed in Fig. 5, and the product $A(P) \times (T^*)^2$ remains approximately pressure independent. These findings correspond to a strongly correlated Fermi-liquid regime at low temperature. We note that the residual resistivity has a weaker pressure dependence than A, but does increase close to the coexistence region. While $A(P)$ cannot be determined precisely below 280 bar, the data suggest a divergency of A at P of order 200 bar, significantly smaller than the pressure at which the extrapolated insulating gap would vanish (of order 370 bar; see above). This suggests that the closure of the Mott-Hubbard gap and the loss of Fermi-liquid coherence are two distinct phenomena, associated with very different energy scales, as is also clear from the fact that the coherence scale T^* (a few tens of Kelvin) is much smaller than the insulating gap Δ (several hundreds Kelvin).

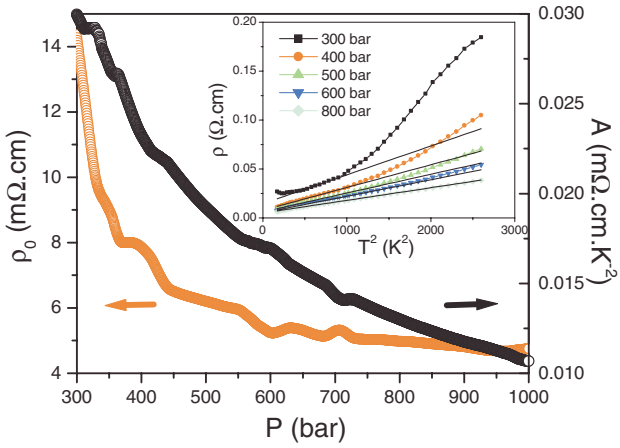

FIG. 5 (color online). Pressure dependence of the T^2 coefficient A and residual resistivity ρ_0. Inset: Plot of ρ vs T^2, also showing the increase of T^* with pressure (straight lines are guides to the eyes).

In order to better characterize the crossover into the bad metal as temperature is increased above T^*, we have performed measurements in a wider temperature range, up to 300 K, as displayed in Fig. 6. We confirm the general behavior reported by other authors [3]. At moderate pressures (a few hundred bars), the resistivity changes from a T^2 behavior below T^* to a regime characterized by very large values of the resistivity (exceeding the Ioffe-Regel-Mott limit by more than an order of magnitude) but still metalliclike ($d\rho/dT > 0$). For pressures in the transition region, this increase persists until a maximum is reached, beyond which a semiconducting regime is entered ($d\rho/dT < 0$). This regime is continuously connected to that found on the insulating side, at temperatures above 50 K. Figure 1 summarizes the four regimes of transport which we have described so far.

We now compare these experimental findings to the DMFT description of the Mott transition. Similarities between DMFT and some physical properties of BEDT organics have been emphasized previously [7,8]. One of

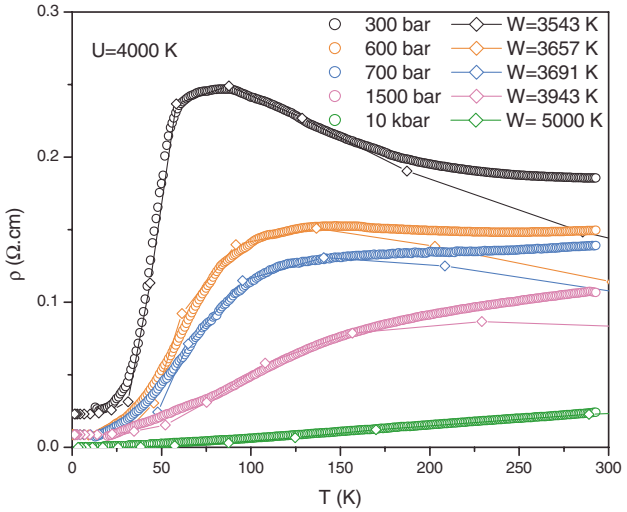

FIG. 6 (color online). Temperature dependence of the resistivity at different pressures. The data (circles) are compared to a DMFT-NRG calculation (diamonds), with a pressure dependence of the bandwidth as indicated. The measured residual resistivity ρ_0 has been added to the theoretical curves.

the key qualitative outcomes of our measurements is the *separation of energy scales* found in the transition region. This is also a distinctive feature of DMFT, in which Hubbard bands are well separated from the quasiparticle peak in the correlated metal, and a coexistence region of insulating and metallic solutions delimited by two spinodal lines is found. The three transport regimes found on the metallic side of the transition are well accounted for within DMFT [2,8–10]. In this theory, a Fermi-liquid regime with long lived quasiparticles applies for T below the coherence scale T^*, with $\rho = AT^2$ and $A \propto 1/(T^*)^2$. As T increases, an intermediate (bad metal) regime is reached, in which the low-energy peak is reduced and strongly temperature dependent, corresponding to a very short lifetime and a large resistivity increasing rapidly with T. As T is further increased, the peak disappears, leaving a pseudogap in the density of states, and a semiconducting transport regime is found, with $d\rho/dT < 0$. We have performed DMFT calculations of the resistivity for a simple Hubbard model at half-filling. The NRG technique was used [11], which is crucial to capture correctly the enhancement of A, and to determine accurately the resistivity maximum. The coupling was fixed at $U = 4000$ K, consistent with the measured critical temperature (within DMFT, $T_c \simeq U/100$). A semicircular band was used, with a bandwidth W adjusted for each pressure, as indicated in Fig. 6. Comparison to the measured $\rho(T) - \rho_0$ involves also a global scale factor (the same for all curves). We find a good agreement between our calculations and the data, up to $T \sim 150$ K, for pressures ranging from the transition (300 bar) to 10 kbar. The fitted bandwidth increases by about 40% in that range. This value, together with the magnitudes of U and W is consistent with theoretical [12] and experimental [13] estimates for these materials. We attribute the discrepancy observed above $\sim$150 K to the strong thermal dilatation of the materials, leading to a smaller effective bandwidth, an effect which could be taken into account by allowing for a T dependence of W in the calculation. The same effect might also contribute to the observed crossover on the insulating side at $T \sim 50$ K, even though DMFT also leads to a similar prediction of a purely electronic crossover at $T \ll \Delta$ [2,9].

Finally, we observe that our data *in the critical regime* around (T_c, P_c) do not appear to obey the critical behavior established within DMFT, namely, that of a liquid-gas transition in the Ising universality class [14]. The observed transition is much too smooth to be described in that manner. Besides the low dimensionality of these compounds, this could be attributed to strong spatial inhomogeneities or disorder in the transition region.

To conclude, we have performed detailed transport measurements on the κ-Cl compound using a variable pressure technique. Four transport regimes have been identified as a function of temperature and pressure, separated by crossover lines. Hysteresis experiments have confirmed the first-order nature of the transition and allowed for the first detailed determination of the coexistence region. DMFT provides a good qualitative description of these crossovers, and new DMFT-NRG calculations of transport are in good agreement with the data. Further theoretical work is needed to understand the critical regime, however. We note that recent ultrasound velocity measurements [6] have revealed anomalies along crossover lines very similar to the two high-temperature lines reported here from transport measurements. This calls for further theoretical work aiming at connecting these two effects.

We are grateful to R. Chitra, V. Dobrosavlevic, G. Kotliar, R. McKenzie, M. Poirier, M. Rozenberg, and A. M. Tremblay for useful discussions. T. A. C., S. F., and A. G. are grateful to KITP-UCSB for hospitality during the final stages of this work (under NSF Grant No. PHY99-07949). T. A. C. acknowledges support from the SFB 195 of the DFG.

[1] M. Imada, A. Fujimori, and Y. Tokura, Rev. Mod. Phys. **70**, 1039 (1998).
[2] For a review, see A. Georges, G. Kotliar, W. Krauth, and M. J. Rozenberg, Rev. Mod. Phys. **68**, 13 (1996).
[3] H. Ito, T. Ishiguro, M. Kubota, and G. Saito, J. Phys. Soc. Jpn. **65**, 2987 (1996), and references therein.
[4] R. H. McKenzie, Science **278**, 820 (1997).
[5] S. Lefebvre, P. Wzietek, S. Brown, C. Bourbonnais, D. Jérome, C. Mèziére, M. Fourmigué, and P. Batail, Phys. Rev. Lett. **85**, 5420 (2000).
[6] D. Fournier, M. Poirier, M. Castonguay, and K. Truong, Phys. Rev. Lett. **90**, 127002 (2003).
[7] R. H. McKenzie, Comments Condens. Matter Phys. **18**, 309 (1998).
[8] J. Merino and R. H. McKenzie, Phys. Rev. B **61**, 7996 (2000).
[9] M. J. Rozenberg, G. Kotliar, and X. Y. Zhang, Phys. Rev. B **49**, 10 181 (1994).
[10] P. Majumdar and H. R. Krishnamurthy, Phys. Rev. B **52**, R5479 (1995).
[11] R. Bulla, T. A. Costi, and D. Vollhardt, Phys. Rev. B **64**, 045103 (2001).
[12] M. Rahal, D. Chasseau, J. Gaultier, L. Ducasse, M. Kurmoo, and P. Day, Acta Crystallogr. Sect. B **53**, 159 (1997).
[13] A. K. Klehe, R. D. McDonald, A. F. Goncharov, V. V. Struzhkin, Ho-Kwang Mao, R. J. Hemley, T. Sasaki, W. Hayes, and J. Singleton, J. Phys. Condens. Matter **12**, L247 (2000).
[14] G. Kotliar, E. Lange, and M. J. Rozenberg, Phys. Rev. Lett. **84**, 5180 (2000).